

PROCEEDINGS OF SPIE

SPIDigitalLibrary.org/conference-proceedings-of-spie

Polarization study in Newtonian telescope components for depolarization parameter correction in atmospheric LiDAR

Estiven Sánchez Barrera, Nairo Torres Fiesco, John Henry Reina Estupiñán

Estiven Sánchez Barrera, Nairo Torres Fiesco, John Henry Reina Estupiñán, "Polarization study in Newtonian telescope components for depolarization parameter correction in atmospheric LiDAR," Proc. SPIE 12537, Laser Radar Technology and Applications XXVIII, 1253708 (12 June 2023); doi: 10.1117/12.2663690

SPIE.

Event: SPIE Defense + Commercial Sensing, 2023, Orlando, Florida, United States

Polarization study in Newtonian telescope components for depolarization parameter correction in atmospheric LiDAR

Estiven Sánchez Barrera^a, Nairo Torres Fiesco^b, and John Henry Reina Estupiñán^c

^aUniversidad Tecnológica de Bolívar, Facultad de Ciencias Básicas, Cartagena, Colombia

^{b,c}Center for Research in Bioinformatics and Photonics - CIBioFi, Universidad del Valle, Cali, Colombia

^cUniversidad del Valle, Departamento de Física, Facultad de Ciencias Naturales, Cali, Colombia

ABSTRACT

In the present work, an experimental system is implemented, and a theoretical model is built that allows quantifying atmospheric depolarization in the city of Santiago de Cali, Colombia. The experimental setup uses a LiDAR coupled to a Polarotor, which allows the separation of the backscattered light into its parallel and perpendicular polarization components. This device allows the use of a single photomultiplier tube, thus facilitating calibration procedures. The theoretical model is based on the Mueller formalism and considers the contribution of each optical element of the LiDAR system on the polarization of the backscattered light. This is achieved by assigning to each element a Mueller matrix and subsequently calculating the matrix associated with the whole assembly. The contribution of the optical elements of the system on the depolarization parameter d is determined. The corrections to the signals obtained are established, so that the data is not altered by the particularities of the assembly used.

Keywords: LiDAR, Depolarization, Aerosols, Atmospheric, Polarization models

1. INTRODUCTION

Currently, there are several methods for monitoring atmospheric phenomena, making use of the variety of ways in which light interacts with small particles, atmospheric aerosols, or molecules. Among these methods, atmospheric LiDAR stands out. LiDAR is an acronym for Light Detection and Ranging and denotes an active remote sensing system based on a laser or coherent radiation beam. Its operating principle is similar to that of radar (radio detection and ranging) and sonar (sound navigation and ranging).¹ This method measures the distance to a target, using the differential time between the emission of a beam of light and the detection of the backscattered part. It is used to make high-resolution maps with applications in geodesy,² archeology,³ geology,⁴ atmospheric physics,^{1,5} and other fields of study. In addition, this technology is also used for the control and navigation of some autonomous cars. For atmospheric measurements with LiDAR, the pulse of light is shot towards the atmosphere, in it, the light is scattered in all directions from the molecules and particles that compose it, a part of this light returns in the direction of the LiDAR and is collected by a telescope and focused on a photodetector.¹ The high resolution, both spatial and temporal, that LiDAR systems allow, as well as the possibility of observing the atmosphere in ambient conditions and the potential to cover a height range of more than 100 km, are reasons why these systems have great appeal for the researchers. The variety of ways in which emitted radiation can interact with atmospheric components allows LiDAR to determine variables such as temperature, pressure, humidity, and wind, as well as trace gases, aerosols, and clouds.⁵

An interesting application of LiDAR systems is the measurement of the rate of depolarization. By means of the polarization components of the backscattered light, it is possible to acquire symmetry parameters of the different particles present in the atmosphere. These measurements allow the identification of various particles such as ash from fires or volcanic eruptions, sand, salt, and some contaminants, making it possible to monitor

Further author information:

E.S.B.: E-mail: barrerae@utb.edu.co

Laser Radar Technology and Applications XXVIII, edited by Gary W. Kamerman,
Lori A. Magruder, Monte D. Turner, Proc. of SPIE Vol. 12537, 1253708
© 2023 SPIE · 0277-786X · doi: 10.1117/12.2663690

Proc. of SPIE Vol. 12537 1253708-1

the intercontinental transport of said compounds.⁶ Depolarization measurements with LiDAR are a technique inherited from analogous measurements with microwave radars, developed in the 1950s before the invention of lasers. Subsequently, it became apparent that, compared to microwave depolarization of non-spherical particles, laser depolarization would be considerably stronger because the particles are generally larger than the wavelengths used.⁵ Despite the importance of this technique, the content referring to the treatment of signals and theoretical models that consider the polarizing effect of the optical elements of the system, as well as theoretical developments that contemplate the use of Polarotors, is incipient. In the present work, a model is proposed for the adjustment of the depolarization component, including the effects associated with optical elements of a LiDAR system with a Newtonian-type telescope and a Polarotor.

2. LIDAR

The basic layout of an atmospheric LiDAR system consists of a transmitter and a receiver. Short pulses of light with a resolution of a few hundred nanoseconds and with specific spectral properties (in our case the laser in the LiDAR-CIBioFi system emits light in a very narrow band around 1064nm, 532nm, or 355nm^{7,8}). Many systems use a beam expander to reduce the divergence of the laser before going out into the atmosphere. In the receiver, a telescope collects the backscattered photons from the atmosphere, followed by an optical analysis system depending on the application. LiDAR used (select desired wavelengths or split beam into respective polarization components). Finally, a receiver module converts said light signal into an electrical one to be stored and processed by a computer.⁵ Figure 1 shows the scheme indicated above.

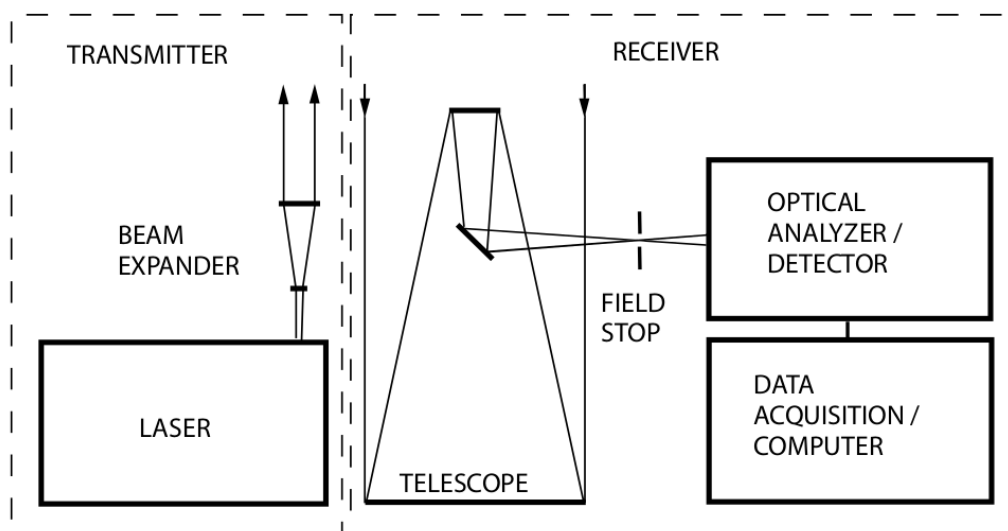


Figure 1. Schematic of the setup of a LiDAR system. Adapted from.⁵

3. POLARIZATION MODEL

An electromagnetic wave can be represented by its electric field component of the form⁹

$$E = E_0 e^{i(kr - \omega t)} \quad (1)$$

If E_0 is constant, the wave is denominated to be polarized. In the case of unpolarized light, the instantaneous polarization fluctuates randomly over time. When light propagates through a medium other than vacuum, the electric field of the waves induces oscillating electric dipoles in the atoms and molecules of said medium, which are the main reason for the optical properties of each substance (refraction, absorption, etc.). Induced dipoles can also scatter light in various directions; the proportion of the light that is scattered will depend on the wavelength of the incident beam, in addition, there is also a polarizing effect in this phenomenon.⁹ The polarization of the scattered light, after the incident on a sample, will depend on several factors; the wavelength in relation to the size

of the sample particles, as well as the shape of these are determining factors. On the other hand, optical elements can transform unpolarized light into linearly polarized light. These devices are known as linear polarizers and there are different types, each of which takes advantage of a different optical phenomenon to eliminate undesired polarization components. In general terms, a polarized electromagnetic wave can be represented in terms of the sum of its real components as

$$\mathbf{E} = E_x \cos(kz - \omega t + \phi_x) \hat{\mathbf{x}} + E_y \cos(kz - \omega t + \phi_y) \hat{\mathbf{y}} \quad (2)$$

Where E_x and E_y are the amplitudes of their components, k is the wave number, ω is the angular frequency, ϕ_x and ϕ_y are the phases of each component, the z - axis corresponds to the propagation axis and the x and y axes will be the equivalent oscillation planes. In cases where ϕ_x and ϕ_y are equal, a linearly polarized wave will be obtained. When the difference between them is a multiple of $\pm\pi/2$ it is called circular polarization, and when the amplitude of the components is not equal or when the phase difference is different from a multiple of $\pi/2$ is called elliptical polarization. A very important concept for the development of this work is partially polarized light, which can be considered as the sum of a component of polarized light and another of unpolarized light; the degree of polarization is defined as the ratio between the polarized component and the total intensity, i.e.

$$P = \frac{I_{pol}}{I_{pol} + I_{nopol}} \quad (3)$$

3.1 Depolarization

Pulsed lasers, generally used in LiDAR systems, produce a linearly polarized light beam, therefore basic applications for polarization in LiDAR include transmission of a light pulse and detection (by means of a beamsplitter) of the backscattered intensity in two perpendicular directions of polarization. The ratio between these two signals, after adjusting for the effect of differences in the optical and electronic gains of the two channels, as well as the polarizing effects of optical instruments and the polarization of ambient light, is called the ratio of linear depolarization or δ value.⁵ Defined in the form:

$$\delta = P_{\perp} / P_{\parallel} \quad (4)$$

where P_{\perp} and P_{\parallel} are the power signals of the perpendicular and parallel polarization components respectively.

This definition is proposed by the pioneers in polarimetric measurements with LiDAR (formerly with Radar) and has been standardized after decades of use.⁵ However, this way of interpreting the polarization loss value can present ambiguities in cases where the polarization loss does not pass from one component to another, but instead, a random polarization occurs. To circumvent these ambiguities, the depolarization parameter d is used, which offers interpretative advantages over measurements, in addition to having a more robust theoretical development.¹⁰ The depolarization parameter d can be defined as

$$d = \frac{2P_{\perp}}{P_{\parallel} + P_{\perp}} \quad (5)$$

It can be rewritten in terms of the coefficient of linear depolarization as

$$d = \frac{2\delta}{1 + \delta}$$

Although these definitions are widely used and their implications have been studied, in this work an adjustment to the depolarization parameter d will be developed, considering the contribution of the optical elements in the possible changes or effects in the detection of the values of P_{\perp} and P_{\parallel} . For that, the Jones and Mueller vectors and matrices will be used.

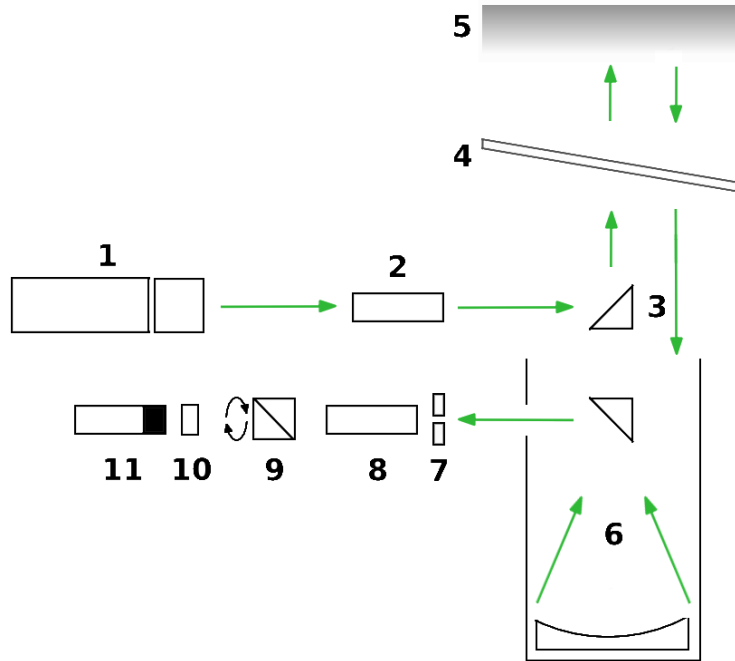


Figure 2. Scheme of the LiDAR setup for depolarization measurement. Its components are **1.** 532 nm laser, **2.** Beam expander, **3.** 45° prism, **4.** Protective glass, **5.** atmosphere, **6.** Newton-type telescope, **7.** Pupil, **8.** Objective lens, **9.** Polarotor **10.** Interference Filter, **11.** Photomultiplier tube.

4. LIDAR SETUP

The LiDAR configuration visible in Figure 2 was used.

The transmission stage of the LiDAR system consists of a Laser (Nd: YAG Quantel Q-smart 450 *mJ* at 532 *nm*), a Galilean-type beam expander with 3*X* expansion, a 45° Quartz prism and a 2° inclined protection glass. After transmission, the backscattered beam passes through the reception stage, which is made up of the protective glass, a Newtonian-type telescope with a focal length of 1 *m*, a primary mirror of 0.3*m* and a field of view of 1.47 *mrad*, pupil or aperture diaphragm of 1*mm*, 25 *mm* objective lens, Polarotor Licel with a Glan-Thompson prism, an interferential filter at 532 *nm* and finally a Hamamatsu R9880U – 20 photomultiplier tube (PMT). As the beam returning from the atmosphere is visible, it passes through multiple optical components that can slightly alter the polarization components. The transformation matrices for each optical component of the receiving system are detailed below.

4.1 Telescope

The transformation matrix of the Newtonian telescope has been obtained based on the works,^{11,12} adjusted to the parameters of the Newtonian telescope used in this work is of the form

$$\mathbf{M}_{Tel} = \begin{pmatrix} 1 & -0.028 & 0 & 0 \\ -0.028 & 1 & 0 & 0 \\ 0 & 0 & 0.977 & 0.210 \\ 0 & 0 & -0.210 & 0.977 \end{pmatrix} \quad (6)$$

4.2 Protective glass and 45° prism

To calculate the Mueller matrix of the prism (40 *mm* PS612 right-angle prism, Thorlabs brand) a beam transformation procedure is carried out in each of the refractive changes and in the internal reflection of the prism;

in this case are obtained two processes of refraction with angle $\theta = 0$ and one reflection with $\theta = 45^\circ$. The refractive index used for this element is quartz, therefore, $n_1 = 1.461^{13}$ for 532 nm, then

$$\mathbf{J}_{Prism} = \begin{pmatrix} t_p(0, n_1) & 0 \\ 0 & t_s(0, n_1) \end{pmatrix} \begin{pmatrix} r_p(\frac{\pi}{4}, n_1) & 0 \\ 0 & r_s(\frac{\pi}{4}, n_1) \end{pmatrix} \begin{pmatrix} t_p(0, \frac{1}{n_1}) & 0 \\ 0 & t_s(0, \frac{1}{n_1}) \end{pmatrix}$$

With Mueller matrix

$$\mathbf{M}_{Prism} = \begin{pmatrix} 1 & -0.401 & 0 & 0 \\ -0.401 & 1 & 0 & 0 \\ 0 & 0 & 0.761 & -0.509 \\ 0 & 0 & 0.509 & 0.761 \end{pmatrix}$$

4.3 Polarotor

In the LiDAR-CIBioFI system, there is a Polarotor Licel that eliminates the need for adjustments due to differences in the optical and electronic gains of the two bias channels. In laboratories where this device is not used, the backscattered light is divided into mutually perpendicular components of polarization with a Polarized beamsplitter (PBS), therefore, a PMT must be positioned in the two directions in which the light is deflected. This separation of the channels is vulnerable to differences in the optical and electronic gains of each channel, the former is understood as the relationship between the transmittance and reflectivity that exists in one component of polarization with the other, this phenomenon will depend on the properties of the PBS: the second one refers to the inconsistencies that the signals generated by each photomultiplier tube could present for an identical radiant flux. These susceptibilities are mitigated by calibrating the system and performing the relevant transformations for each signal.^{14,15} Now, consider that the PBS is not fixed; the laser is shot and its light is backscattered toward the receiving system, it passes through the PBS and one of its components is isolated; while the laser charges its next shot is rotated the PBS 90° when is generated a new pulse and the backscattered light passes through the PBS, it will isolate one of its polarization components, this time in a perpendicular direction. Therefore, if the PBS is rotated 90° each time the laser shot a new pulse, a single PMT could be used to measure two perpendicular polarization components; it is enough to store in a different memory all pulses in which the PBS was in one direction or another. The advantage of this procedure is, firstly, to always use the same optical path for both polarization directions, this eliminates optical differences; then, it eliminates the possible electronic differences of using multiple PMTs. In essence, the polarotor works with this procedure; it is essentially a PBS that rotates at a constant angular velocity, such that, it makes a quarter of a revolution in the time between one laser pulse and the next. Since the Polarotor is, in essence, a rotating polarizer, its representation in the Mueller formalism is

$$\mathbf{Pol}(\phi) = \mathbf{LP}(\theta - \theta_0) \quad (7)$$

Where ϕ is the angle measured from the x-axis of the reference frame that we choose and θ is the adjustment angle of the laser shot and signal reception. \mathbf{LP} corresponds to the Mueller matrix of a Linear polarizer of the form

$$\mathbf{LP}(\theta) = \frac{1}{2} \begin{pmatrix} 1 & \cos(2\theta) & \sin(2\theta) & 0 \\ \cos(2\theta) & \cos^2(2\theta) & \sin(2\theta)\cos(2\theta) & 0 \\ \sin(2\theta) & \sin(2\theta)\cos(2\theta) & \sin^2(2\theta) & 0 \\ 0 & 0 & 0 & 1 \end{pmatrix} \quad (8)$$

The optimal adjustment angle for separating the system's perpendicular and parallel polarization components was obtained through a signal sweep, varying the angle and comparing the signals obtained. In the end, was obtained a value of $\theta = 52.11^\circ \pm 0.7^\circ$.

5. MEASUREMENT AND QUANTIFICATION OF THE DEPOLARIZATION PARAMETER

It is possible to model the optical path of the light emitted by the laser and subsequently backscattered by the atmosphere with the following sequence of Mueller matrices

$$\mathbf{M}_{tot}(z) = \mathbf{Pol}(\phi(z)) \cdot \mathbf{M}_{Tel} \cdot \mathbf{M}_{Glass} \cdot \mathbf{M}_{atm}(z) \cdot \mathbf{M}_{Glass} \cdot \mathbf{M}_{Prism} \quad (9)$$

where all the matrices used have been previously developed. The \mathbf{M}_{atm} matrix that represents the atmosphere, refers to an optical element that depolarizes an incident beam, also inverts some directions of the original reference frame because it has been considered that the light is reflected in the direction of the telescope. However, it is necessary to consider that this matrix must be defined for each spatial coordinate in the atmosphere, therefore, the parameter d varies from one point to another, additionally a parameter must be added that accounts for the loss of light intensity along the route. This is how we can define the following matrix

$$M_{atm}(z) = Atm(z) \begin{pmatrix} 1 & 0 & 0 & 0 \\ 0 & 1 - d(z) & 0 & 0 \\ 0 & 0 & d(z) - 1 & 0 \\ 0 & 0 & 0 & 2d(z) - 1 \end{pmatrix}$$

with

$$\lim_{z \rightarrow \infty} Atm(z) = 0$$

For an initial polarized beam represented as a Stokes vector $\mathbf{S} = (1, 1, 0, 0)$, is possible calculate the signal produced by both channels as

$$P_{\parallel}(z) = Atm(z)[0.291 + 0.008 d(z) + (0.291 - 0.299 d(z)) \cos 2\phi(z)] \quad (10)$$

$$P_{\perp}(z) = Atm(z)[0.291 + 0.008 d(z) - (0.291 - 0.299 d(z)) \cos 2\phi(z)] \quad (11)$$

After some algebraic manipulations, the depolarization parameter d can be calculated as

$$d_c(z) = \frac{1.161P_{\perp}(z) - 0.003P_{\parallel}(z)}{0.613P_{\parallel}(z) + 0.579P_{\perp}(z)} \quad (12)$$

Is been defined d_c in equation 12 as the corrected depolarization parameter to compare with the d (uncorrected) parameter in equation 5. Figure 3 shows the curves for the depolarization measurements shown so far (equations 4, 5 and 12) as a function of the signal ratio P_{\perp}/P_{\parallel} ; note that there is a considerable difference with δ , since it is obtained through a different formalism.

As for d and d_c there is no considerable difference. However, this small difference can be representative when evaluating materials with very similar degrees of depolarization.

6. CONCLUSIONS

The use of techniques for measuring the depolarizing capacity of the atmosphere as a method of identifying atmospheric phenomena in the city of Cali, and even in the Colombian southwest, is an aspect on which there is no precedent. In this work, a detailed theoretical model has been built for the determination of the depolarization parameter d , which serves to quantify the depolarizing capacity of the particles present in the atmosphere. This development is within the formalism of the Mueller calculation, so the individual contributions of the optical elements of the system have been considered, in order to determine the corrections to be made in the signal processing, with respect to the standard definition of the parameter.

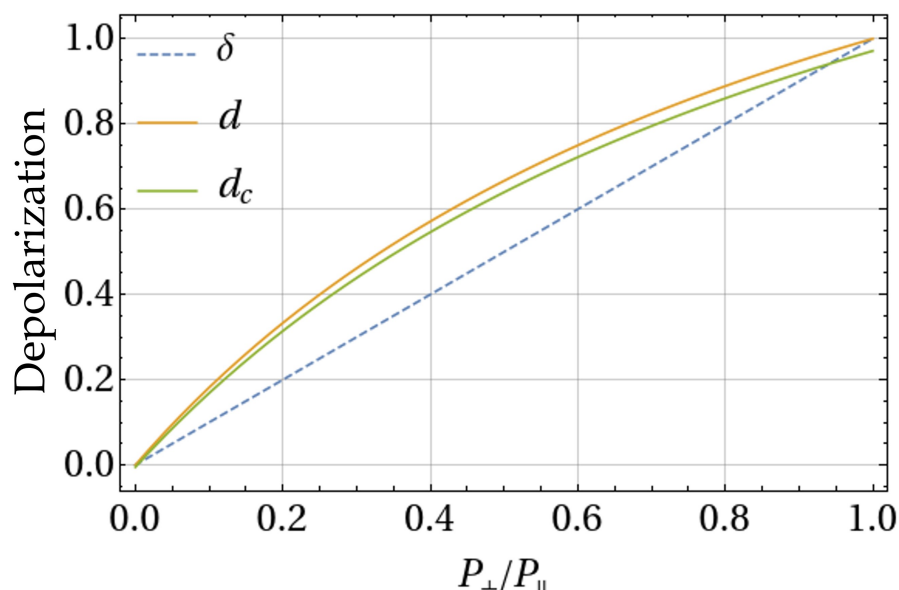


Figure 3. Measurements of depolarization according to different definitions. The dotted blue line represents the linear depolarization ratio, and the orange curve is the depolarization parameter d , without making any corrections based on the polarizing effects of the system. Finally, the green curve represents said parameter after making the corresponding corrections.

ACKNOWLEDGMENTS

The author thanks the Center For Bioinformatics and Photonics CIBioFi and the “Ministerio de Ciencia y Tecnología MINCIENCIAS” from Colombia through the program “4DAir-MOLIS”.

REFERENCES

- [1] Eichinger, V. A. K. . W. E., [*Elastic Lidar*], John Wiley & Sons, Ltd (2005).
- [2] Glennie, C., Carter, W., Shrestha, R., and Dietrich, W., “Geodetic imaging with airborne lidar: The earth’s surface revealed,” *Reports on progress in physics. Physical Society (Great Britain)* **76**, 086801 (07 2013).
- [3] Chase, A. S. Z. and Chase, Diane Z. and Chase, A. F., [*LiDAR for Archaeological Research and the Study of Historical Landscapes*], 89–100, Springer International Publishing, Cham (2017).
- [4] Burton, D., Dunlap, D., Wood, L., and Flaig, P., “Lidar intensity as a remote sensor of rock properties,” *Journal of Sedimentary Research - J SEDIMENT RES* **81** (05 2011).
- [5] Milonni, P. W., “Lidar. range-resolved optical remote sensing of the atmosphere, in the springer series in optical sciences, vol. 102, edited by claus weitkamp,” *Contemporary Physics* **50**(5), 19–40 (2009).
- [6] et al, T. M., “Application of lidar depolarization measurement in the atmospheric boundary layer: Effects of dust and sea-salt particles,” *Journal of Geophysical Research: Atmospheres* **104**(D24), 31781–31792 (1999).
- [7] Rojas, J. C., *Implementación de un sistema LiDAR elástico para la observación de la dinámica de aerosoles sobre el área urbana de Cali*, Master’s thesis, Universidad del Valle, Escuela de Ingeniería de los Recursos Naturales y el Ambiente (EIDENAR) (6 2019).
- [8] D.R. Vivas, E. Sánchez, J. R., “Deep learning the atmospheric boundary layer height.,” *Remote Sensing* (2020).
- [9] Hecht, E., [*Optics*], Pearson Education, Incorporated (2017).
- [10] Gimmestad, G. G., “Reexamination of depolarization in lidar measurements,” *Appl. Opt.* **47**, 3795–3802 (Jul 2008).
- [11] Di, H., Hua, D., Yan, L., Hou, X., and Wei, X., “Polarization analysis and corrections of different telescopes in polarization lidar,” *Appl. Opt.* **54**, 389–397 (Jan 2015).

- [12] Sanchez Almeida, J. and Martínez-Pillet, V., “Instrumental polarization in the focal plane of telescopes,” *Astronomy and Astrophysics* **260**, 543–555 (06 1992).
- [13] Malitson, I. H., “Interspecimen comparison of the refractive index of fused silica*,†,” *J. Opt. Soc. Am.* **55**, 1205–1209 (Oct 1965).
- [14] et al, F., “Depolarization ratio profiling at several wavelengths in pure saharan dust during samum 2006,” *Tellus B* **61**, 165 – 179 (02 2009).
- [15] Freudenthaler, V., “About the effects of polarising optics on lidar signals and the $\delta 90$ calibration,” *Atmospheric Measurement Techniques* **9**(9), 4181–4255 (2016).